

## Article

# Machine-Learning-Based Ground-Level Mobile Network Coverage Prediction Using UAV Measurements

Naser Tarhuni <sup>\*</sup>, Ibtihal Al Saadi, Hafiz M. Asif, Mostefa Mesbah, Omer Eldirdiry and Abdulnasir Hossen

Department of Electrical &amp; Computer Engineering, Sultan Qaboos University, Muscat 123, Oman

\* Correspondence: tarhuni@squ.edu.om

**Abstract:** Future mobile network operators and telecommunications authorities aim to provide reliable network coverage. Signal strength, normally assessed using standard drive tests over targeted areas, is an important factor strongly linked to user satisfaction. Drive tests are, however, time-consuming, expensive, and can be dangerous in hard-to-reach areas. An alternative safe method involves using drones or unmanned aerial vehicles (UAVs). The objective of this study was to use a drone to measure signal strength at discrete points a few meters above the ground and an artificial neural network (ANN) for processing the measured data and predicting signal strength at ground level. The drone was equipped with low-cost data logging equipment. The ANN was also used to classify specific ground locations in terms of signal coverage into poor, fair, good, and excellent. The data used in training and testing the ANN were collected by a measurement unit attached to a drone in different areas of Sultan Qaboos University campus in Muscat, Oman. A total of 12 locations with different topologies were scanned. The proposed method achieved an accuracy of 97% in predicting the ground level coverage based on measurements taken at higher altitudes. In addition, the performance of the ANN in predicting signal strength at ground level was evaluated using several test scenarios, achieving less than 3% mean square error (MSE). Additionally, data taken at different angles with respect to the vertical were also tested, and the prediction MSE was found to be less than approximately 3% for an angle of 68 degrees. Additionally, outdoor measurements were used to predict indoor coverage with an MSE of less than approximately 6%. Furthermore, in an attempt to find a globally accurate ANN module for the targeted area, all zones' measurements were cross-tested on ANN modules trained for different zones. It was evaluated that, within the tested scenarios, an MSE of less than approximately 10% can be achieved with an ANN module trained on data from only one zone.

**Keywords:** network coverage; machine learning; drone systems



**Citation:** Tarhuni, N.; Al Saadi, I.; Asif, H.M.; Mesbah, M.; Eldirdiry, O.; Hossen, A. Machine-Learning-Based Ground-Level Mobile Network Coverage Prediction Using UAV Measurements. *J. Sens. Actuator Netw.* **2023**, *12*, 44. <https://doi.org/10.3390/jsan12030044>

Academic Editors: Jawad Rasheed, Adnan M. Abu-Mahfouz, Asadullah Shaikh, Amir Masoud Rahmani and Gerhard P. Hancke

Received: 18 April 2023

Revised: 18 May 2023

Accepted: 23 May 2023

Published: 26 May 2023



**Copyright:** © 2023 by the authors. Licensee MDPI, Basel, Switzerland. This article is an open access article distributed under the terms and conditions of the Creative Commons Attribution (CC BY) license (<https://creativecommons.org/licenses/by/4.0/>).

## 1. Introduction

People depend more and more on their mobile wireless devices for their daily activities. Hence, one of the primary goals of modern cellular network operators is to ensure high-quality coverage in both urban and rural areas. To do so, they regularly evaluate their services to assess how well the signal is received by the user. This information is required to better adapt their networks to the needs and demands of their users and to plan for future deployments. There are several ways to assess signal strength in a specific area, such as specialized software that uses topological information and network users' reports or user complaints. Field measurement campaigns are, however, the most reliable way to assess coverage quality. Walking or driving through target areas and using specialized equipment, such as multichannel receivers and GPS trackers, are key methods that can be deployed for the collection of field measurement data [1]. This approach is, however, not suitable for remote and hard-to-access areas. An alternative is to use UAVs for this purpose. This method recently became very attractive due to its efficiency, low cost, and safety. Drones can be used to reduce human involvement and the risk of accidents during

measurement campaigns, particularly in difficult-to-reach areas. Drones were primarily utilized for simple tasks like security, aerial photography, or videography, but they can now function as flying network nodes. One or two drones acting as network nodes will increase the system's capacity and the network's coverage [2]. The drones' relatively high-altitude flying, with respect to the ground base, is one issue to consider when measuring network coverage. Antennas mounted on towers and buildings are tilted down toward the ground to improve reception. However, signal strength at higher altitudes differs from that received at ground level. Machine learning (ML) algorithms have been used as an efficient solution to this problem [3]. Artificial intelligence (AI) algorithms, which is a subset of machine learning (ML), can predict signal strength at ground level given signal strength measurements at high altitudes. ML enables the learning of complex relationships between variables in complex environments that are difficult to express mathematically. Deep learning algorithms, one of the many types of machine learning algorithms, have recently surpassed human performance in a number of engineering applications [4].

Estimating mobile signal strength using ANN and data collected by a drone was initially investigated in [3]. The multilayer perceptron neural network (MLP-NN) was used to generate a dense 2D map of mobile signal strength at the ground level.

In this paper, we investigate the use of drone measurements taken from fixed altitudes above the ground in an open area to predict signal strength at an angle with respect to target location at ground level. The collected data were also used to estimate the signal strength within a building in the same area. The use of limited measurement data is also discussed. Additionally, we used the measurements at different on-campus zones to develop one ANN module to predict the signal strength with acceptable accuracy at other locations.

The paper is organized as follows. Section 2 reviews the related work. Section 3 explains the methodology and measurement procedures for data acquisition. Section 4 presents the analysis and the structure of the ANN module. The results are presented and discussed in Section 5. Finally, the conclusion and future work are discussed in Section 6.

## 2. Related Work

Nguyen et al. [5] studied the quality of mobile coverage in rural areas by collecting signal strength measurements at varying altitudes using a drone. The authors noticed that as a drone ascended 120 m above the ground, the signal loss increased from 4.2% to 51.7%, and that the interference intensified, limiting the coverage quality. The drone experiences more interference because path loss increases with altitude and approaches free space.

Amorim et al. [6] used an LTE scanner attached to a drone to measure mobile signal strength. The authors found that the propagation environment is significantly different for airborne UAVs and ground-level users. To account for the dependence on the height/altitude, they proposed a modified a height-dependent alpha-beta (AB) model [7]. The reference signal received power (RSRP) was utilized to indicate the signal strength in a specific area and estimate the network coverage area. Nekrasov et al. [8] employed various techniques to collect RSRP readings. Using an application on a mobile phone attached to a drone at various altitudes was one such technique. The authors found a poor correlation between measurements collected by a drone and those collected on the ground. In terms of signal strength, they categorized the RSRP into five classes ranging from excellent to poor. The results demonstrated that the data collected by the drone were 72% more accurate compared to the data collected on the ground.

The authors of [9] examined various estimation techniques used to enhance network connectivity and quality of service (QoS). One of these techniques applied an ANN to enhance the receiver and transmitter designs. The link distance, altitude, frequency, and path loss were the inputs to the ANN. The output provided an estimate of the received signal strength on the ground from the flying drone. The results demonstrated that the ANN produced accurate predictions of the received signal strength. This result was also confirmed by [10]. In [11,12], an ANN was used to predict the signal strength. The authors trained the ANN using measurements collected from a UAV. The primary objective of the

work was to design an optimal model of the strength of the signal received by the drone. The input to the neural network includes the latitude, longitude, the elevation of both the drone and the cell building, and the antenna mast’s height. The output was the estimated signal strength at the location of the drone. In an urban setting, the signal strength data and elevation were used as inputs to an ANN. The output was a vector indicating the type of environment in which the measurements were taken, and the environment’s channel parameters were accurately estimated using this information.

### 3. Measurement Methodology

A layout of the measurement system procedures is shown in Figure 1. A phone equipped with the application is attached to the drone. The drone path was defined by the drone controller, and the measurement application was set to record the required information. The drone started the mission, and after returning back to its set location, the recorded data were used for post-processing. The post-processing includes several steps, such as data cleaning, normalization and classification. The post-processed data were used to train the selected ANN. Then, new data from the same drone path or from other paths, zones, and buildings were applied to the trained ANN for testing.

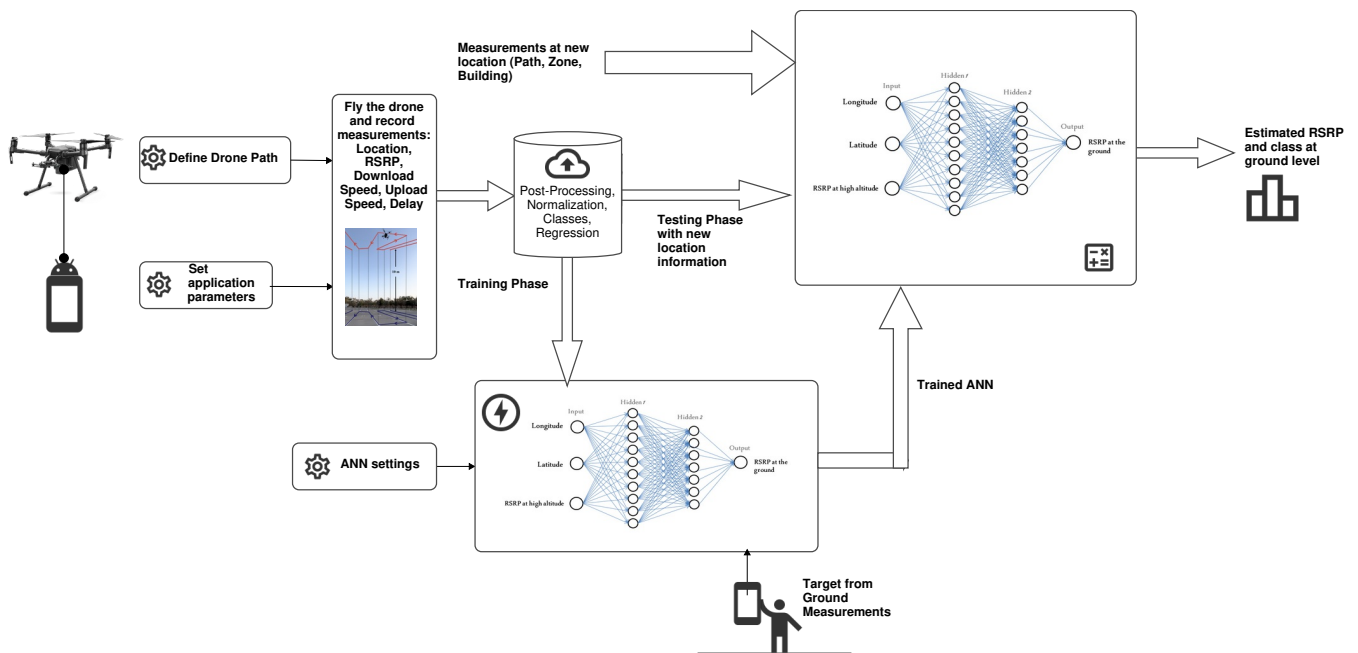


Figure 1. Measurement procedure.

The measurements were conducted in 12 areas within Sultan Qaboos University’s campus. Figure 2 depicts a map of SQU campus, with the targeted zones highlighted by yellow pushpins. Some of these regions were open spaces with fewer obstacles (Zones 1, 7, 9, 11, and 12), streets (Zone 10), near or between buildings (not shown on the figure), some agriculture areas (Zones 2, 3 and 8), and parking lot areas (Zones 4, 5 and 6). The path loss is generally proportional to distance  $d$  according to  $d^{-n}$ , where the path loss exponent  $n$  is  $\approx 2$  in open areas and  $\approx 4$  near streets and buildings. The procedure for collecting measurements was similar across all sites. In this section, we present the methods used to collect the data at various altitudes and on the ground.



**Figure 2.** Location of the measurement locations within the SQU campus.

#### *Air/Ground Data Measurement*

A drone is a remotely piloted flying robot that follows a predetermined flight path. Drones are able to cover large geographic areas that traditional drive or walk tests cannot [13]. They can be used to assess signal strength in rural and urban areas at higher altitude and to transmit collected data to a processing center to check the service quality of the signal [8]. The DJI Matrice 200 V2 quadcopter was used in this study. It is a high-quality commercial drone. The Matrice 200 V2 has 17-inch propellers that are attached to powerful motors to ensure stable flight, even in strong winds. Moreover, it has a dual-battery setup for longer flight time. Due to its adaptability and durability, it has been used in various applications. The drone weighs 3.8 kg and has a maximum payload of 2.3 kg and a maximum flight time of 24 min. Its flight maximum range is 7 km. An off-the-shelf smartphone was used to record the signal strength and GPS coordinates. The smartphone was equipped with an application that can read a variety of mobile network parameters. G-NetTrack, a driving test and network monitor application for 2G, 3G, and 4G networks able to detect multiple LTE channels, served as the mobile receiver in cases where there was no LTE network connection. The measured parameters were logged during the test time and kept in a file for post-processing. The smartphone was mounted on the drone, and the application was configured to measure the signal strength, network delay, and upload and download data speeds, along with the location information. In this work, we used only the signal strength and location information for prediction. Before each flight, the application was set to start recording manually and measure new reading sets of parameters every second. This could be changed in the application settings to record more readings in smaller areas. The drone's altitude remained constant throughout each flight to estimate signal strength on the ground using data recorded at high altitudes. The desired height was measured relative to the ground at the point of takeoff. Using the drone controller, the altitude was fixed to a certain height, and with autopilot mode, the drone had such high stability that it could fly horizontally along the path. The drone maintained constant altitudes (10 m, 18 m, and 24 m) throughout its different flights.

According to [14], a back-and-forth pattern, which is subdivided into parallel and creeping lines, is preferable when the covered area is large and the likely target meeting point is unknown. The path followed by the drone is depicted in Figure 3. The yellow location pin indicates the takeoff and return points of the drone. The blue and white circles indicate the selected targeted area, which is approximately  $50 \times 52 \text{ m}^2$  in size. The green circle is the point where the drone starts flying in the target area. The white lines show the path pattern followed by the drone at the three altitudes. The drone was programmed to travel at  $1 \text{ m/s}$  throughout the designated area. This speed was found to be the best option to allow the application to take as many readings as possible. On average, the drone required about five minutes to collect the data. This period could be changed depending on the size of the covered zone. However, the majority of the zones are about  $50 \times 50 \text{ m}^2$  in size. The period of the process was kept to a minimum because our approach was used to compensate or make up for the time spent performing drive/walk tests. To optimize the efficiency and precision of the system, changes could easily be made to the drone's speed, the size of the areas, and the interval between drone data acquisitions.

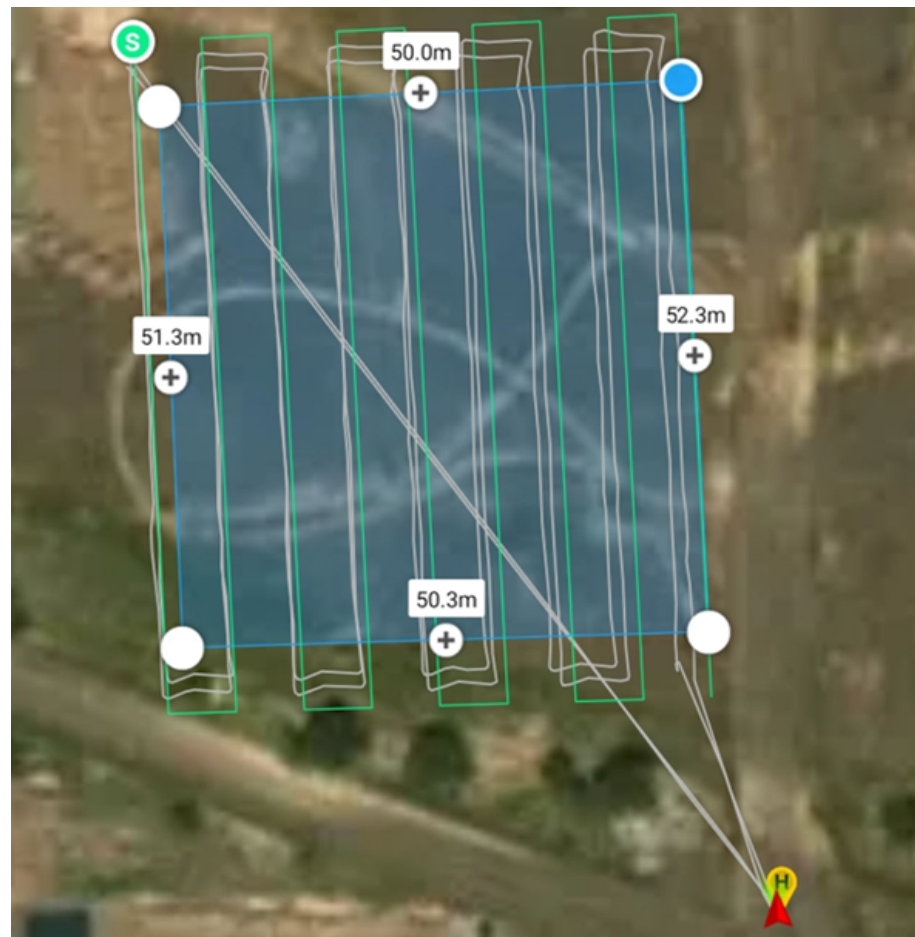
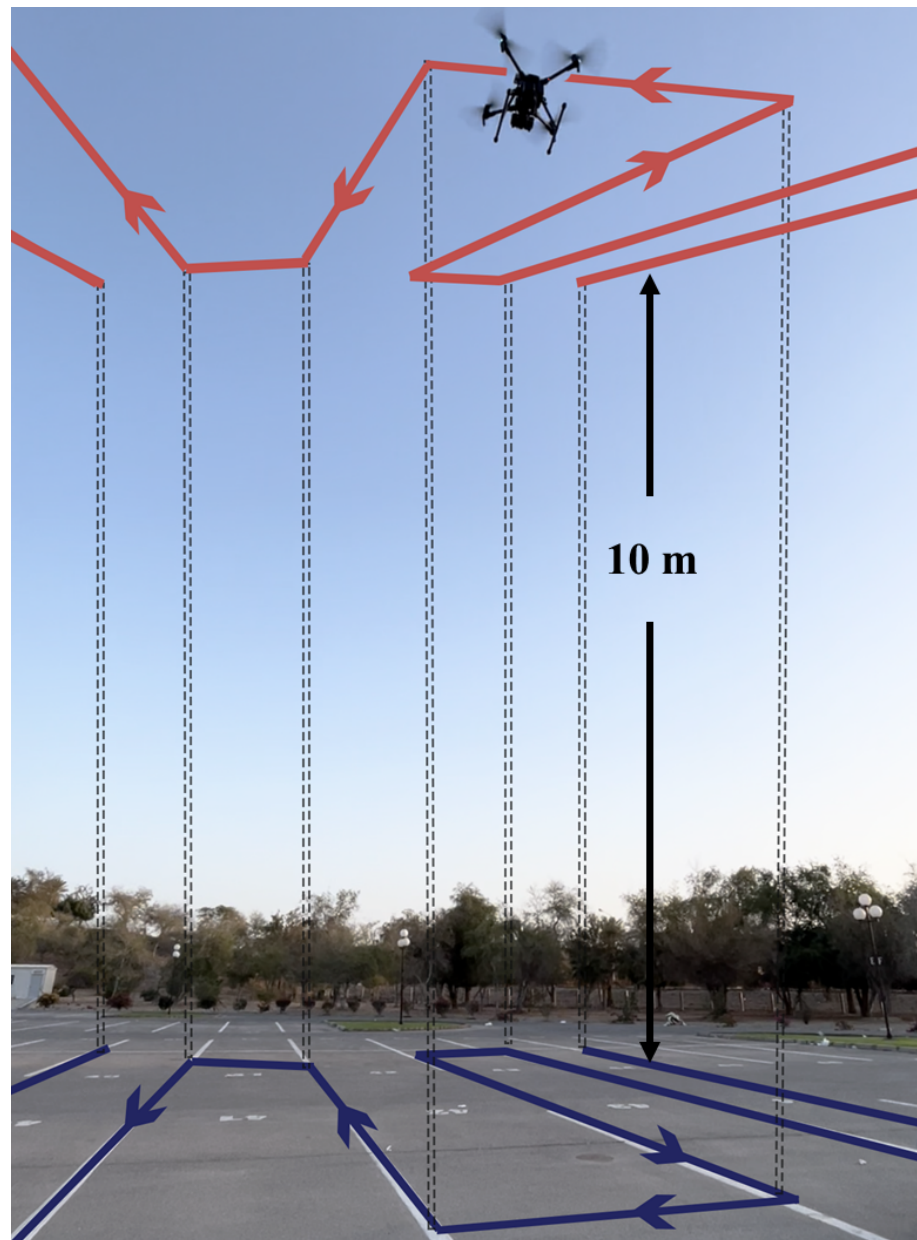


Figure 3. Drone flight pattern.

Identifiable objects were positioned at specific locations along the drone's path used to collect signal strength measurements. The signal strength was also collected at these locations on the ground using the same application settings. Figure 4 depicts the path of the drone and the corresponding path on the ground.



**Figure 4.** Drone flight and ground measurement paths.

#### **4. Data Analysis**

This section details the methods for analyzing and processing raw recorded measurements, choosing the neural network structure, and estimating signal strength.

##### *4.1. Data Pre-Processing*

The number of measured points for data collected on the ground and in the air at various altitudes differ. All the data were initially aligned according to their GPS locations. Although the flight path of the drone was predetermined, measurements at different altitudes and on the ground were not necessarily taken at the exact same GPS coordinates. This step involved omitting misaligned information from the collected measurements. The collected measurements for all altitudes and each location were plotted graphically to check the positioning of the measured points along the path. The farthest points from the path were omitted. Figure 5 depicts the locations where measurements were taken initially prior to cleaning, and locations where measurements were taken following cleaning are shown in Figure 6.

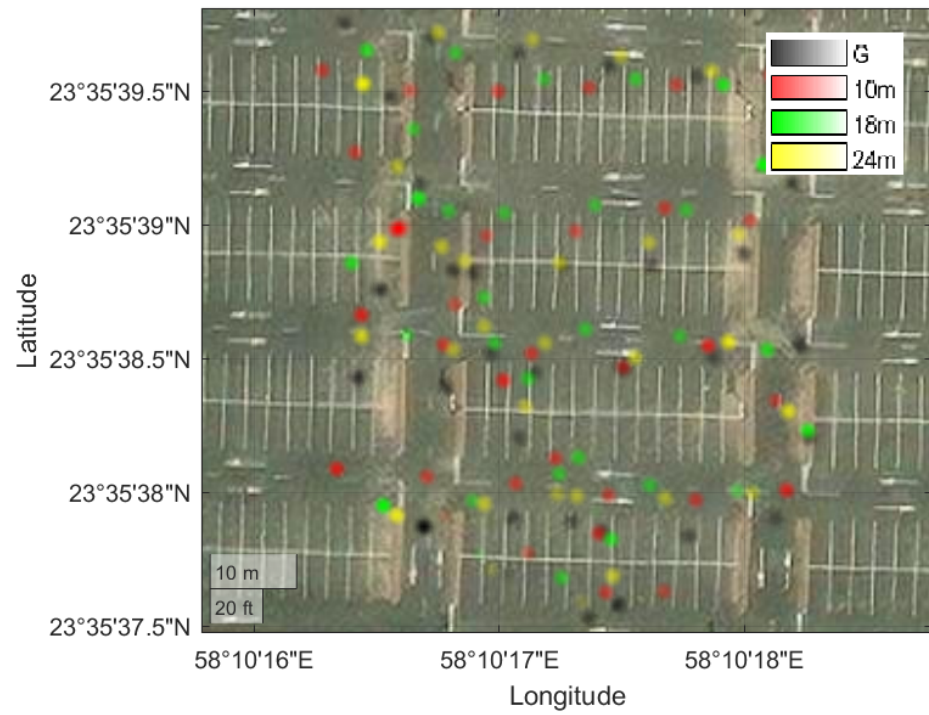


Figure 5. Measurement location before data cleaning.

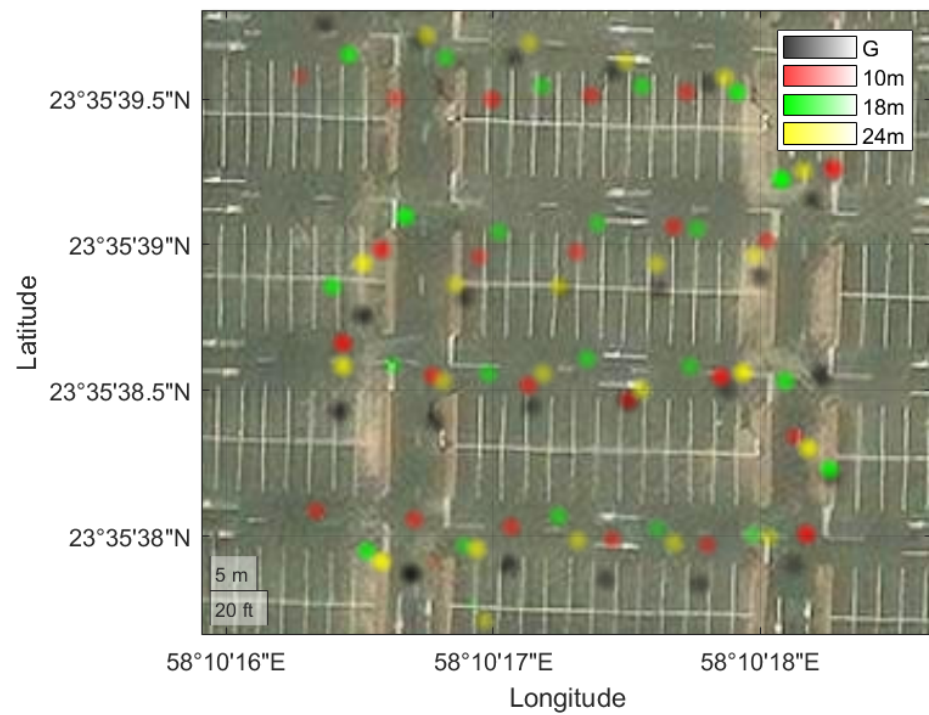


Figure 6. Measurement location after data cleaning.

The measured data and location information to be applied to the ANN varied in magnitude. In order to improve the accuracy of the ANN output and accelerate the learning process, the input and output variables of the ANN were normalized [15]. To accomplish this, the following min/max equation was utilized:

$$X'_n = \frac{X_n - \min(X_n)}{\max(X_n) - \min(X_n)} \quad (1)$$

where  $X_n$  is the original non-normalized data and  $X'_n$  is the normalized data. The reverse process can be used to recover the non-normalized result.

#### 4.2. Structuring the Artificial Neural Network

An ANN module is conventionally composed of a number of layers [16], including one input layer, an output layer, and one or more hidden layers. In this work, the inputs to the ANN module were the longitude and latitude location of the measurements and the signal strength measured at high altitudes (in dBm). Measurements were conducted at various heights in order to analyze the effects of altitude on the prediction accuracy and to determine the optimal height. The output of the ANN was the predicted ground-level RSRP. The collected data were separated into three sets. The training set (70%) was used to train the ANN, the validation set (20%) was used to prevent overfitting, and the test set (10%) was used to evaluate the performance of the trained ANN. The test set, which was entirely distinct from the training set, was randomly selected from the entire dataset. The number of iterations (epochs) used to train the ANN was set to 500. Mean square error (MSE) is frequently used to evaluate the performance of a trained model for the regression problem and is expressed as

$$\text{MSE} = \frac{1}{n} \sum_{i=1}^n (P_i - \hat{P}_i)^2 \quad (2)$$

where  $n$  represents the number of test data,  $P_i$  represents the actual test values, and  $\hat{P}_i$  represents the predicted test values. In this work, the MSE target for the network was set to 0.001. When the MSE reaches the target value or the number of predefined epochs has passed, model training ceased.

To our knowledge, there is no simple rule or standard formula for determining the number of hidden layers and the number of neurons in each layer. Incorrectly determining these parameters can sometimes lead to conditions known as overfitting and underfitting, which have a very negative impact on the network's efficiency and time complexity. Having a large number of neurons in the first hidden layer is, therefore, an acceptable starting point. The number of neurons on the other layers should decrease and converge to that of the output layer [17]. Regarding the number of hidden layers, we started with one layer, then increased the number of layers to twenty. Each time, the model was trained with a different number of neurons. For each number of hidden neurons, the MSE was calculated, as well as its impact on the prediction accuracy. With ten neurons, we achieved acceptable performance on the test data set. Consequently, 10 neurons were chosen for the first hidden layer. Similar steps were taken for the second hidden layer. An MLP-NN with two hidden layers of 10 neurons in the first layer and 7 neurons in the second layer was adopted after several trial-and-error steps. Figure 7 depicts the architecture of the adopted ANN.

ANNs can be configured to predict signal strength using two distinct methods: regression and classification. The ANN's output is a numerical value representing the predicted RSRP in regression. In contrast, the output of classification is a number that indicates the category of the signal level as one of four classes (due to the level of coverage quality), as shown in Table 1. In this paper, we used ANN regression to attempt to predict the exact value of RSRP.

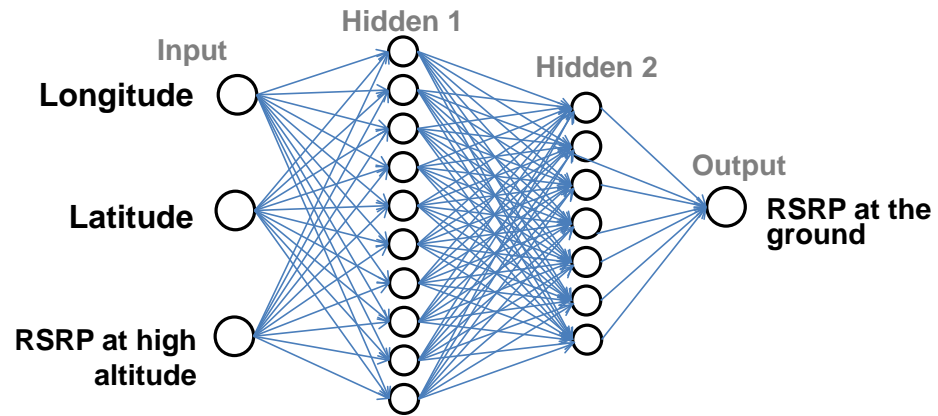


Figure 7. Structure of the Neural Network: 2 Hidden layers, 1 output layer, 17 neurons.

Table 1. Signal strength quality classifications.

RSRP Range (dBm)	RSRP Quality	Color
>−90	Excellent	Green
−90 to −105	Good	Yellow
−106 to −120	Fair	Orange
<−120	Poor	Red

### 5. Results and Discussion

In this section, several measurement setups will be discussed, including ground-level drive tests, drone-based predictions, outdoor-to-indoor predictions, predictions from drone data at an angle, and cross-zone predictions.

#### 5.1. Drive-Test Approach

Before putting our approach to the test with the drone, we tested several scenarios to predict RSRP at ground locations using measurements from other ground locations. This was accomplished by driving a vehicle around the campus while recording the location and RSRP readings along the route. This test employed the same hardware/software setup that was used for air measurements.

Then, we attempted to estimate the signal strength along the same path but at distinct locations. These distinct points that were used for testing were different from the points that were used for training and had not been seen by the neural network. The same proportion of data was divided into three groups as before. In this case, the only input to ANN was the location points (longitude and latitude), and the estimated RSRP was the output. To easily visualize the signal quality at a particular location, we plotted a map displaying the predicted RSRP after training (see Figure 8). According to Table 1, green points indicate excellent coverage, while yellow points indicate good coverage. The predicted RSRP is shown in Figure 9, including the error bar showing less scattering in most locations and indicating a good prediction performance. Alternatively, the error histogram in Figure 10 reveals that the majority of predicted RSRP are close to actual measurements. The horizontal coordinate represents the MSE error for the testing test, and the vertical coordinate (instances) represents the number of samples from the dataset. The average percentage of error was determined to be 3.7%.

In this classification method, the target output is the predicted class of the test data’s signal strength, as stated in Table 1. The input to the neural network was only the location (longitude and latitude), and the output was the estimated class. The data were divided into three groups in proportions of 70:10:20 for training, validation, and testing, respectively. The measurements were found to only include 3 ranges of classes (excellent, good, and fair); there were no poor signals found, and therefore, the NN did not predict the class ‘Poor’

for any output. However, the results of the classification algorithm showed an accuracy of 92.2%. The confusion matrix shown in Figure 11 depicts the percentage of the prediction performance of the classifier. The green squares indicate the correct predictions for each class, and the red squares indicate the wrong predictions. For example, in the first green square, 85 test measurements of the ‘excellent’ class were predicted correctly, with 65.9% overall accuracy. The bottom squares represent the accuracy and the error prediction of each class. For the ‘good’ class, the NN successfully predicted 86.8% of signals that fell into this signal strength category and failed to predict the other 13.2%.

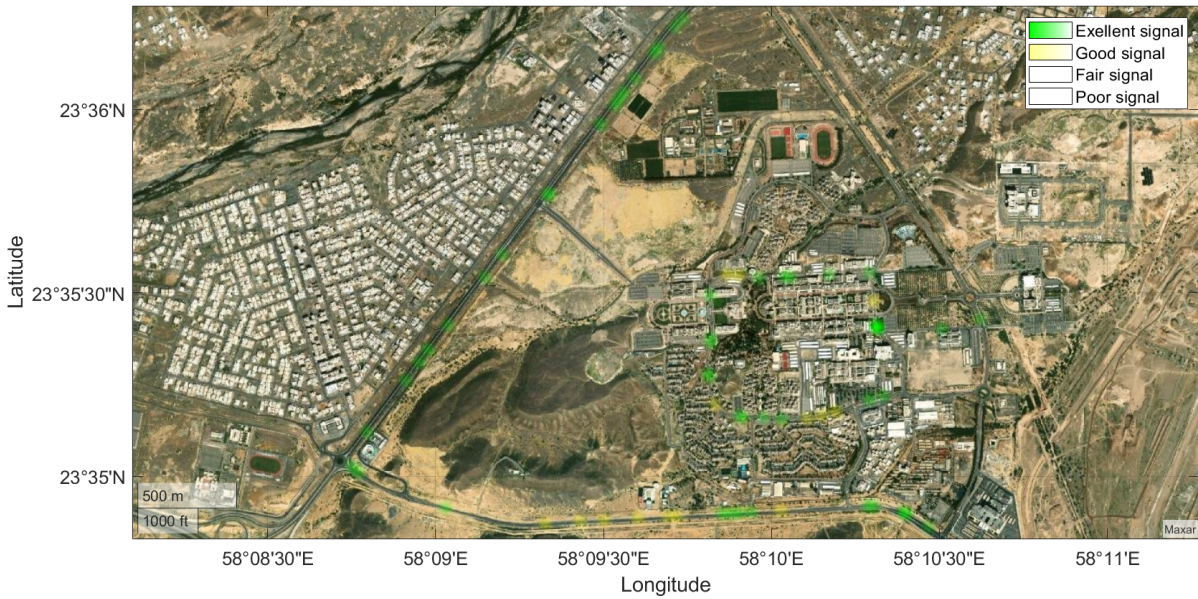


Figure 8. Drive test locations.

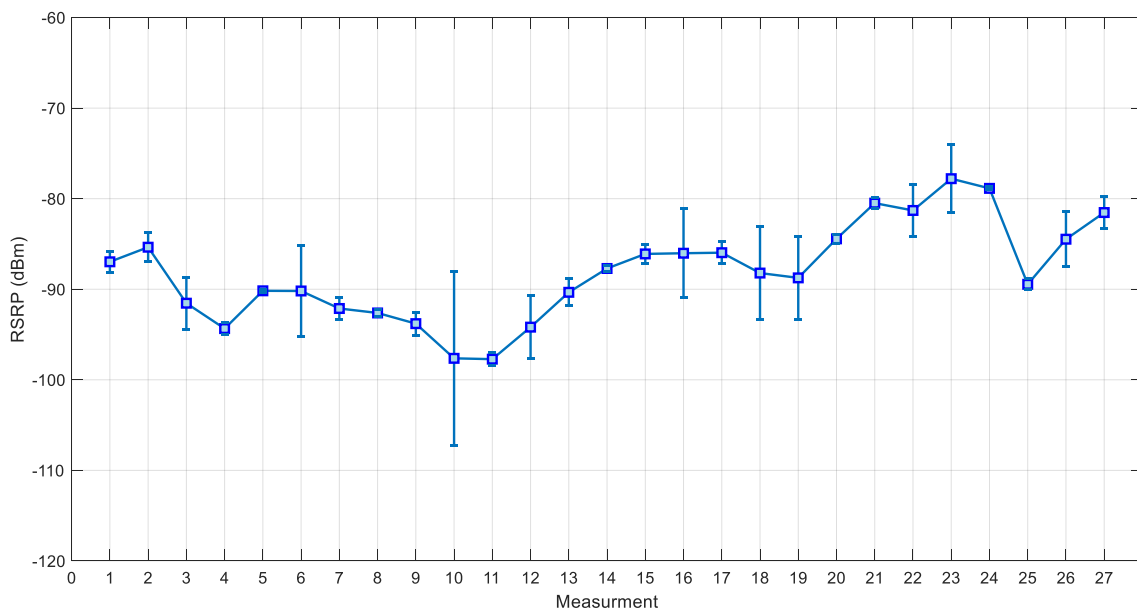


Figure 9. The predicted RSRP and error bar.

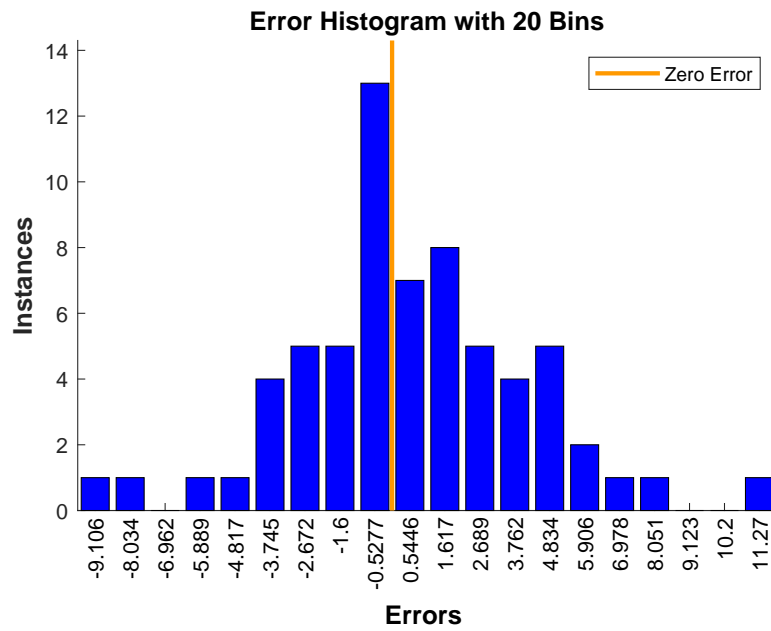


Figure 10. RSRP prediction error histogram.

	Excellent	Good	Fair	
Excellent	85 65.9%	4 3.1%	0 0.0%	95.5% 4.5%
Good	4 3.1%	33 25.6%	1 0.8%	86.8% 13.2%
Fair	0 0.0%	1 0.8%	1 0.8%	50.0% 50.0%
	95.5% 4.5%	86.8% 13.2%	50.0% 50.0%	92.2% 7.8%
	Excellent	Good	Fair	Target Class

Figure 11. Confusion matrix for test location RSRP classification.

### 5.2. Drone Flight Results

As previously stated, the ground signal strength at the same geolocation points was estimated in our work. In this regard, we made use of RSRP measurements at altitudes of 10 m, 18 m, and 24 m, respectively. Figure 12 (right) shows the path followed by the drone and a grid of measurement points at 10 m height. At the beginning of the training procedure, the MSE was high in the first epoch; however, this decreased throughout training until it reached its lowest value for the validation set. Figure 12 (left) shows the estimated results of the test locations within the collected dataset. Table 2 consists of some significant parameters used in our experiment, i.e., a sample of the test set locations, the percentage error of the estimated signal strengths relative to the actual error, the actual ground measurements, and the ANN-based estimated RSRPs. The average MSE error was determined to be approximately 3%.

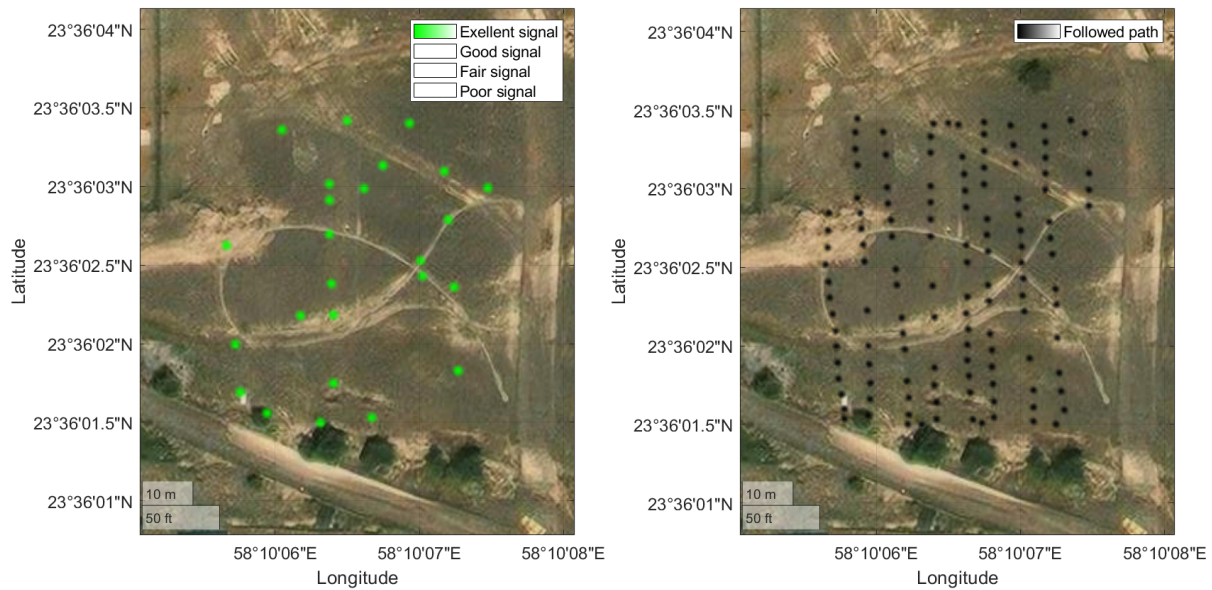


Figure 12. Drone path (right) and the predicted RSRP (left).

Table 2. Sample of test results.

Longitude	Latitude	Measured RSRP, dBm	Estimated RSRP, dBm	Error, %
58.1683	23.6005	−77.1000	−75.5050	2.0687
58.1683	23.6005	−76.6000	−74.9638	2.1361
58.1683	23.6005	−76.1000	−75.8127	0.3775
58.1683	23.6007	−76.8000	−74.7034	2.7300
58.1684	23.6007	−76.0000	−76.8867	1.1667
58.1684	23.6006	−76.7000	−77.8693	1.5245
58.1684	23.6005	−77.7000	−76.6334	1.3727
58.1684	23.6008	−75.6000	−72.7632	3.7524

The same method was applied to measurements collected at 18 m and 24 m altitudes. The neural network was trained again with the measurements collected at each location and RSRPs at 18 m and 24 m altitudes to predict the signal strength on the ground. Only measurements of one altitude were used for training and testing each time. All three altitudes provided accurate predictions of RSS on the ground. The MSE was 3.9%, 4.2%, and 4.5% for 10 m, 18 m, and 24 m, respectively. Consequently, predictions based on the tested altitudes yield acceptable results, with approximately 0.5% difference. When selecting the optimal altitude to predict the signal strength of the ground, multiple factors must be taken into consideration. One of them is selecting a path with no obstacles that could potentially damage the drone. As a result, we flew our drone above surrounding obstacles (e.g., streetlights and trees). Even though we were unable to fly the drone above 25 m due to authority regulations, we did observe signal degradation at these altitudes in certain locations.

### 5.3. Impact of Location Area

Geographical locations and terrain characteristics impact signal strength predictions. Due to several factors, urban areas, for instance, are more complex than free-space areas. RSRP is also affected by channel impairments, such as attenuation, reflection, and shadowing. These factors appear to occur more frequently in dense urban areas due to tall buildings and other obstacles. Figures 13 and 14 depict an agricultural region and an open area region, respectively. We applied the trained ANN to both locations to predict RSRP on

the ground and to observe the effect of location. Therefore, the average MSE of agricultural locations was determined to be 2.8 dB, while that of open space was determined to be 2.4%. The applied ANN has an average accuracy of approximately 97% for all locations, regardless of area clutter.

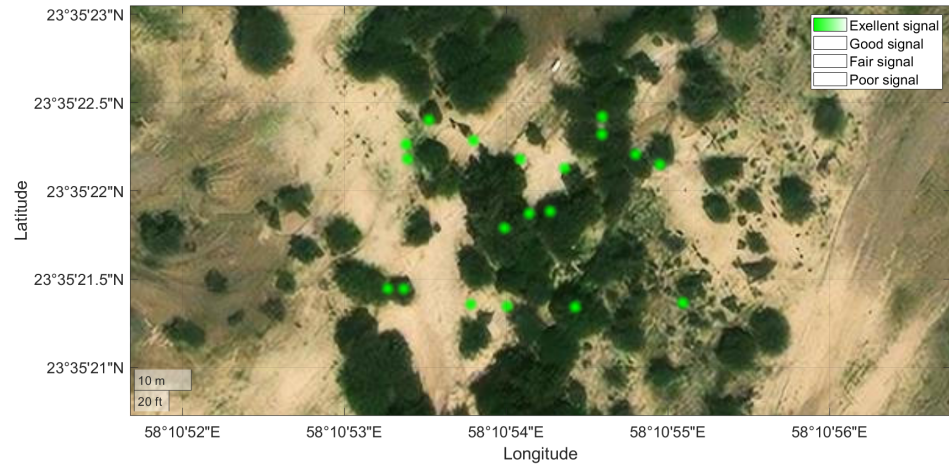


Figure 13. Estimated RSRP on agriculture location.

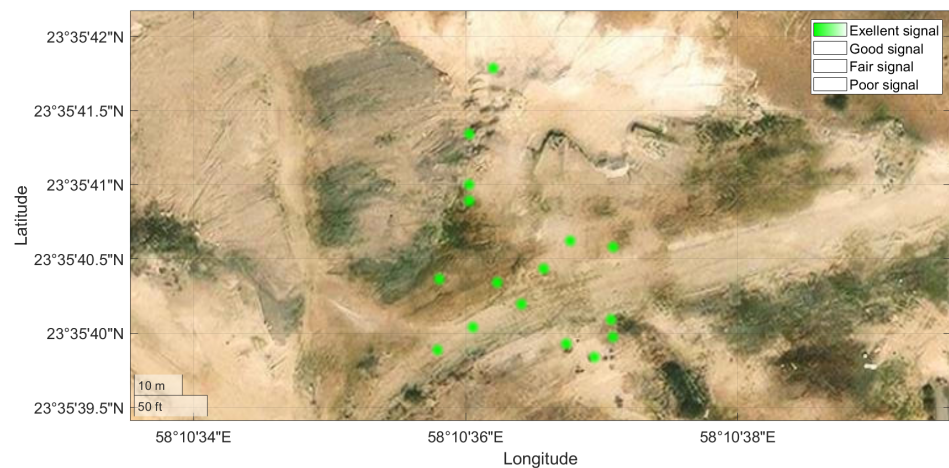


Figure 14. Estimated RSRP on open area location.

All previous scenarios predicted the signal strength of the same location point on the ground relative to the signal strength at a high altitude. Due to obstacles such as trees, mountains, or other obstructions, it is sometimes impossible to conduct a drone or drive test to measure signal strength at high altitudes or on the ground along the target path. Therefore, it serves the same purpose to fly the drone at an angle. In this scenario, we explore the possibilities for predicting the signal strength from a drone at a specific angle. To examine the effect of different angles on signal strength prediction, the height of the drone was fixed at 10 m. Location and RSRP data collected at 10 m altitude were inputs to the ANN, and the output was the RSRP on the ground at an angle with respect to the vertical. Figure 15 depicts the flight path of the drone and the predicted RSRP on the ground at an angle of 32 degrees and 68 degrees from the drone. The percentage MSE was determined to be 2.3% for angles closer to the drone and 2.6% for those further away. Overall, it appears that both cases accurately predict signal strength on the ground.

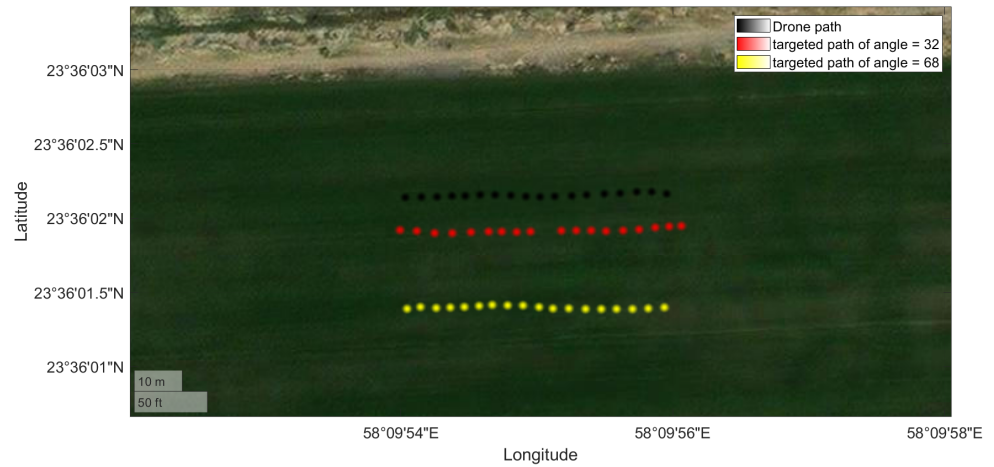


Figure 15. Drone path and targeted test paths of different angles from the drone.

The neural network could also predict the signal strength of a path with a previously unseen angle and measurements of another different angle. In this instance, the neural network structure included the angle value as an input. The training set consisted of the data for the path directly beneath the drone (angle = 0) and the path within an angle (68° in the tested scenario) from the drone. The test set consisted of a path between these two ground-level angles. Figure 16 depicts the system’s outline. The red points represent the routes included in the network’s training set. The blue point represents the predicted target RSS of the path between two red points. The percentage MSE was determined to be 1.58%. Hence, it is possible to use the trained ANN to predict the signal strength on the ground with different angles from the drone, which can be useful if there are difficulties measuring the signal strength due to the drone’s limits or restrictions regarding the location. Table 3 displays a sample of the test outcomes.

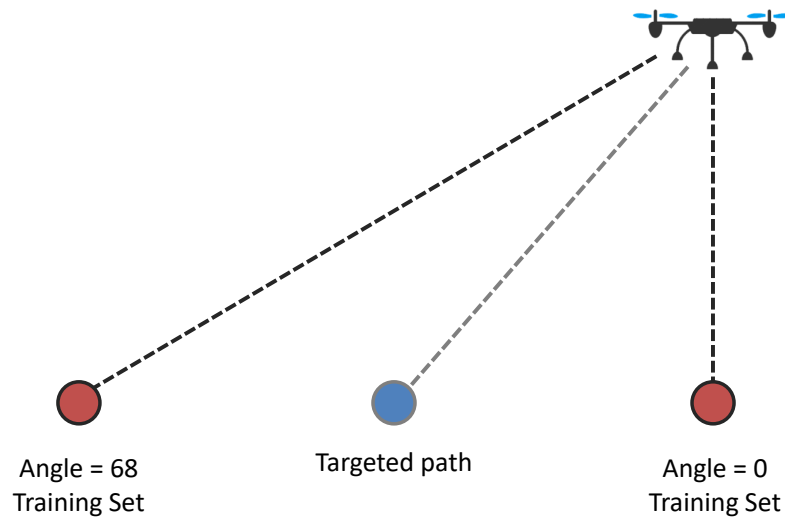


Figure 16. Outline of the training scenario with angle information.

Table 3. Sample of test results with angle measurements.

Longitude	Latitude	Measured RSRP, dBm	Estimated RSRP, dBm	Error, %
58.1650	23.6005	−79.8000	−79.0407	0.9515
58.1651	23.6005	−80.5000	−79.7568	0.9233
58.1651	23.6005	−79.3000	−79.2822	0.0225

Table 3. Cont.

Longitude	Latitude	Measured RSRP, dBm	Estimated RSRP, dBm	Error, %
58.1651	23.6005	−79.7000	−78.3743	1.6633
58.1652	23.6005	−78.5000	−78.3233	0.2251
58.1652	23.6005	−78.3000	−78.5976	0.3801
58.1652	23.6005	−80.2000	−78.1301	2.5809

5.4. Outdoor–Indoor Signal Prediction

One of the efficient and time-saving ways to measure signal strength inside buildings is to use the signal levels measured outside the building. This can be applied to high-rise buildings by measuring the signal using a drone to predict the coverage inside the building. Here, we tested the situation using ML to predict signal strength without the need to physically walk through each building. This depended on a variety of factors, such as the building’s structure, which could consist of typical cement with metal rods or other materials. In addition to the walls, the objects and the distance from the base station could weaken the signal’s ability to propagate through the building. Furthermore, the frequency of operation can also impact the behavior of the signal’s propagation through the building. We tested the outdoor–indoor prediction scenario within the university campus in different buildings. The location and RSRP values outside the building were given as inputs to the neural network, and the predicted RSRP values inside the building were estimated. The MSE error for testing within the same building was determined to be 2.28% with location information and 5% without location information. Next, the trained ANN module was utilized to predict the signal strength in another building. Walk tests were conducted inside and outside the building to evaluate the trained model’s accuracy. It was determined that the trained ANN module accurately predicted the signal strength with an acceptable error rate of 5.4%. Figure 17 depicts the tested building scenario. Figure 18 displays the predicted RSRP for the same building and a different building, as well as the error bar for each case. Next, the trained ANN module was applied to estimate RSRP within a third building with a different structure and design. The building was a workshop with a wide, open area and a different indoor structure as compared to the office building used for training. The MSE of the estimated RSRP in this new case jumped to 24%.



Figure 17. Path within second building.

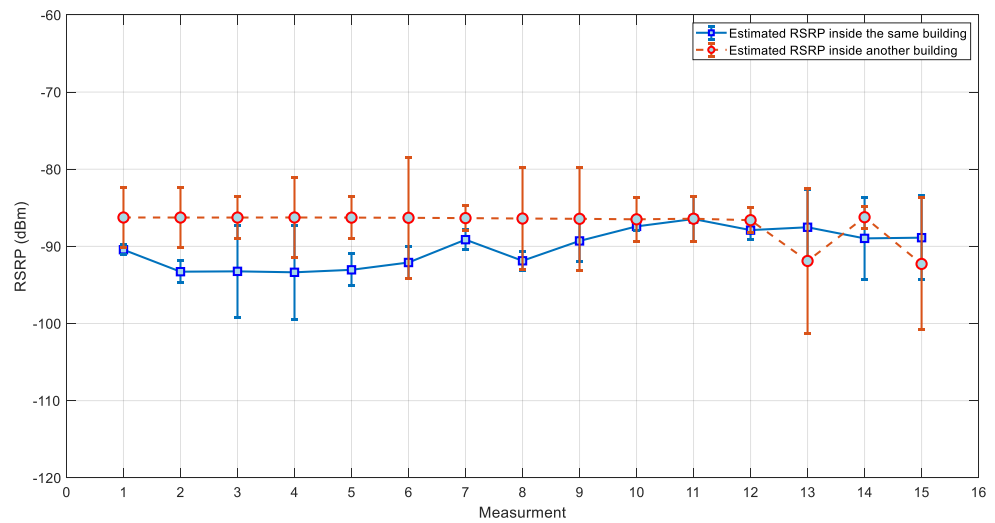


**Figure 18.** Predicted indoor RSRP and error bar using outdoor measurements.

### 5.5. Cross-Zone Prediction

Although it is theoretically possible to determine the strength of an electromagnetic field at any given location in space using the Maxwell equations, the amount of data and level of precision required make it practically impossible. The signal strength was predicted with the aid of a model that simplified the calculations. There are many available models for this, such as the Okumura–Hata and COST models. To predict the signal strength or the path loss, these models require distinct types of environments and operational information, such as frequency of operation, Tx and Rx antenna parameters, TX–RX distance, and type of clutter. On the other hand, the method used in this work requires location information and a trained ANN module. Twelve trained ANN modules were developed for the twelve tested campus zones. These trained modules were used to test newly collected data from other zones without retraining the network. To accomplish this, we considered the collected measurement for each zone to be a new piece of information for each trained ANN module. In total, eleven new measurements were attempted on each module. While it is impossible to predict signal strength with absolute certainty, the results indicate that the average error was minimized when the training zone was close to the test zone (for example, zone 1 and zone 2) and/or the RSRP ranges of the two zones are comparable. Overall, this method could be enhanced by including additional input data, such as the transmitted power from the base station or the path loss. Figure 19 depicts the MSE prediction error matrix after testing the trained ANN module with new data from other locations for all zones. The blue squares indicate that each zone is evaluated using its own test data. The green squares indicate good predictions with lower MSEs based on the results of the predicted RSRPs and how closely they match the actual RSRP. It was expected to have an MSE of less than 7%. Yellow squares indicate an acceptable prediction range of 7% to 15% MSE. Red squares represent poor predictions, with an MSE greater than 15%. As depicted in the figure, the module trained on zone 7 data provided the most accurate prediction for all other zones tested on campus. Consequently, it can serve as a default model for predicting the signal strength inside the university using a drone. The model trained on zone 4 cannot be used as the default model because it predicts the weakest signal strength for all campus test data. This is believed to be due to the fact that zone 4 was close to the base station antenna, with strong signals and less variability.

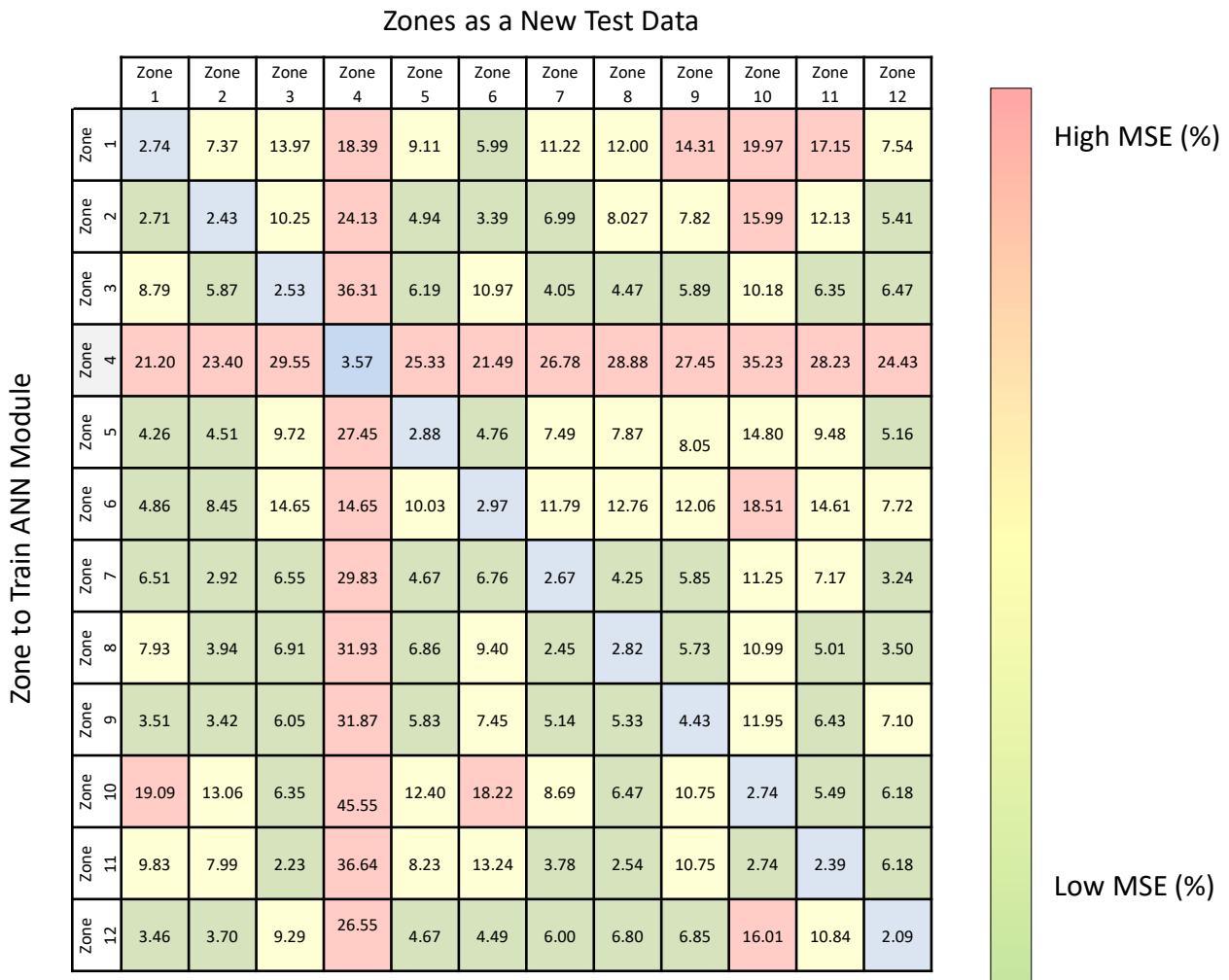


**Figure 19.** MSE prediction between different zones.

### 5.6. Training Set Size

Drones in general have short battery life, and on the other hand, there is a need to reduce the effort put forth while taking field measurements. It is essential to specify the minimum percentage of the training class that would show acceptable results. Here, we examined the impact of reducing the training set’s size on the accuracy of the signal estimation. Instead of using the default division of 70:20:10 for training:validating:testing, different division values were tried for these classes. The chart in Figure 20 shows the average and the maximum error for using different values for the testing set, ranging from 90% until 20%. The error increases as the size of the testing set grows, as expected. However, the average error drops to less than 5% when testing with less than 80% of the data.

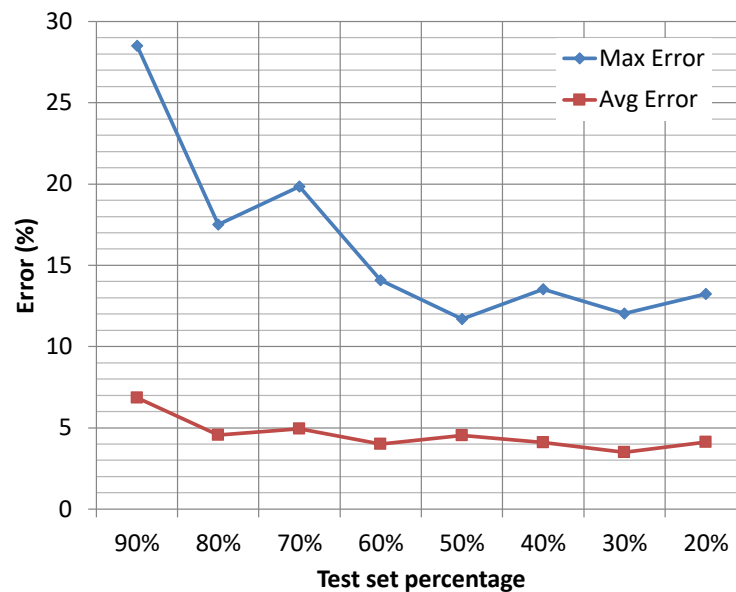


Figure 20. Impact of training set size on prediction MSE.

## 6. Challenges and Future Work

Several challenges may limit drone-based drive test systems, including the need for permission to fly drones in certain areas and altitude restrictions imposed by authorities. Due to these constraints, measurements for this study were conducted only on campus, and the maximum height was set at 25 m. Another challenge is identifying a suitable machine learning (ML) algorithm that can work in multiple wireless propagation environments. In this study, we selected ANNs because of their flexibility in updating their parameters and their ability to model complex scenarios. Finding one network for all environments might be challenging. However, a simple solution is to use multiple trained ANN networks for different scenarios. On the other hand, other ML approaches should also be investigated. Candidate ML algorithms should be investigated and ranked using formal methods to verify the correctness of the chosen ML algorithm. Formal methods are a set of mathematical techniques that can be used to verify the correctness, security, and fairness of software systems [18,19]. However, there are also some challenges to the application of formal methods to machine learning and AI. Machine learning models are often complex and non-linear, which can make them difficult to verify using formal methods. Additionally, the data used to train machine learning models are often noisy and incomplete, which can also make it difficult to verify the correctness of these models.

## 7. Conclusions

In this paper, we used drone measurements from higher altitudes to predict ground-level coverage. The method utilized an ANN module trained mainly with the measured signal strength at higher altitude and the location data of the targeted point at ground level. Several zones on the campus of Sultan Qaboos University, Oman, were used to collect data. At each measurement zone, the trained module accurately predicted the signal level with acceptable precision. In addition, the module trained for each zone was used to predict the ground-level signal strength in other zones. For the tested scenarios, it was found that training an ANN module in one zone can be used to predict the signal strength in other zones with an error of 10%. Additionally, outside measurements were used to predict the signal strength inside of buildings. This emulates the scenario of using drone measurements taken from outside a high-rise building to predict coverage inside the building.

**Author Contributions:** Conceptualization, N.T. and M.M.; methodology, N.T. and I.A.S.; software, I.A.S.; validation, N.T. and H.M.A.; formal analysis, N.T. and I.A.S.; investigation, I.A.S.; resources, N.T.; data curation, O.E. and A.H.; writing—original draft preparation, I.A.S.; writing—review and editing, N.T., M.M., A.H. and H.M.A.; project administration, N.T. and A.H. All authors have read and agreed to the published version of the manuscript.

**Funding:** This research was funded by Omantel grant no. (EG/SQU-OT/21/01), Sultanate of Oman, under the research project “Mobile Network Coverage Assessment using Unmanned Aerial Vehicle and Artificial Intelligence”.

**Institutional Review Board Statement:** Not applicable.

**Informed Consent Statement:** Not applicable.

**Data Availability Statement:** Not applicable.

**Acknowledgments:** The authors would like to thank Embedded & Interconnected Vision Systems Laboratory at Sultan Qaboos University for contributing to drone measurements.

**Conflicts of Interest:** The authors declare no conflict of interest.

## References

1. Song, L.; Shen, J. *Evolved Cellular Network Planning and Optimization for UMTS and LTE*, 1st ed.; Virtual Drive Test; CRC Press: Boca Raton, FL, USA, 2010; pp. 80–85.
2. Athanasiadou, G.E.; Batistatos, M.C.; Zarbouti, D.A.; Tsoulos, G.V. LTE ground-to-air field measurements in the context of flying relays. *Wirel. Commun.* **2019**, *26*, 12–17. [\[CrossRef\]](#)
3. Saadi, I.A.; Tarhuni, N.; Mesbah, M. Ground Level Mobile Signal Prediction Using Higher Altitude UAV Measurements and ANN. In Proceedings of the 32nd Conference of Open Innovations Association (FRUCT), Tampere, Finland, 9–11 November 2022; pp. 15–21.
4. Lin, X.; Wiren, R.; Euler, S.; Sadam, A.; Maattanen, H.L.; Muruganathan, S.D.; Gao, S.; Wang, Y.-P.E.; Kauppi, J.; Zou, Z.; et al. Mobile Network-Connected Drones: Field Trials, Simulations, and Design Insights. *IEEE Veh. Technol. Mag.* **2019**, *14*, 115–125. [\[CrossRef\]](#)
5. Nguyen, H.C.; Amorim, R.; Wigard, J.; Kovacs, I.Z.; Mogensen, P. Using LTE Networks for UAVCommand and Control Link: A Rural-Area Coverage Analysis. In Proceedings of the 2017 IEEE 86th Vehicular Technology Conference (VTC-Fall), Toronto, ON, Canada, 24–27 September 2017; pp. 1–6.
6. Amorim, R.; Nguyen, H.; Mogensen, P.; Kovacs, I.Z.; Wigard, J.; Sørensen, T.B. Radio channel modeling for UAV communication over cellular networks. *Wirel. Commun. Lett.* **2017**, *6*, 514–517. [\[CrossRef\]](#)
7. Rappaport, T. *Wireless Communications: Principles and Practice*; Prentice-Hall: Upper Saddle River, NJ, USA, 2002.
8. Nekrasov, M.; Adarsh, V.; Paul, U.; Showalter, E.; Zegura, E.; Vigil-Hayes, M.; Belding, E. Evaluating LTE Coverage and Quality from an Unmanned Aircraft System. In Proceedings of the IEEE 16th International Conference on Mobile Ad Hoc and Sensor Systems (MASS), Monterey, CA, USA, 4–7 November 2019; pp. 171–179.
9. Alsamhi, S.H.; Ma, O.; Ansari, M.S. Predictive estimation of the optimal signal strength from unmanned aerial vehicle over internet of things using ANN. *arXiv* **2018**, arXiv:1805.07614.
10. Tomasevic, N.M.; Neskovic, A.M.; Neskovic, N.J. Artificial neural network based simulation of short-term fading in mobile propagation channel. In Proceedings of the Telecommunications Forum Telfor (TELFOR), Belgrade, Serbia, 25–27 November 2014; pp. 206–212.
11. Goudos, S.K.; Tsoulos, G.; Athanasiadou, G. Artificial neural network optimal modelling of received signal strength in mobile communications using UAV measurements. In Proceedings of the 12th European Conference on Antennas and Propagation (EuCAP 2018), London, UK, 9–13 April 2018; pp. 1–4.
12. Goudos, S.K.; Tsoulos, G.V.; Athanasiadou, G.; Batistatos, M.C.; Zarbouti, D.; Psannis, K.E. Artificial Neural Network Optimal Modeling and Optimization of UAV Measurements for Mobile Communications Using the L-SHADE Algorithm. *IEEE Trans. Antennas Propag.* **2019**, *76*, 4022–4031. [\[CrossRef\]](#)
13. Nekrasov, M.; Allen, R.; Belding, E. Performance Analysis of Aerial Data Collection from Outdoor IoT Sensor Networks using 2.4 GHz 802.15.4. In Proceedings of the 5th Workshop on Micro Aerial Vehicle Networks, Systems, and Applications, MobiSys’19, Seoul, Republic of Korea, 21 June 2019; pp. 33–38.
14. Andersen, H.L. Path Planning for Search and Rescue Mission Using Multicopters. Master’s Thesis, Institutt for Teknisk Kybernetikk, Trondheim, Norway, 2014.
15. Demuth, H.; Beale, M.; Hagan, M. *Neural Networks Toolbox™ User’s Guide*; The Mathworks Inc.: Natick, MA, USA, 2009; 1992–2009, Online Only, Revised for Version 6.0.3.
16. Razafimandimby, C.; Loscri, V.; Vegni, A.M. A neural network and IoT-based scheme for performance assessment in Internet of Robotic Things. In Proceedings of the 2016 IEEE First International Conference on Internet-of-Things Design and Implementation (IoTDI), Berlin, Germany, 4–8 April 2016; pp. 241–246.

17. Hassoun M.H. Fundamentals of artificial neural networks. *Proc. IEEE* **1996**, *84*, 906. [[CrossRef](#)]
18. Raman, R.; Gupta, N.; Jeppu, Y. Framework for Formal Verification of Machine Learning Based Complex System-of-Systems. *INSIGHT* **2023**, *26*, 4022–4031. [[CrossRef](#)]
19. Krichen, M.; Mihoub, A.; Alzahrani, M.Y.; Adoni, W.Y.H.; Nahhal, T. Are Formal Methods Applicable To Machine Learning And Artificial Intelligence? In Proceedings of the 2nd International Conference of Smart Systems and Emerging Technologies (SMARTTECH), Riyadh, Saudi Arabia, 9–11 May 2022; pp. 48–53.

**Disclaimer/Publisher's Note:** The statements, opinions and data contained in all publications are solely those of the individual author(s) and contributor(s) and not of MDPI and/or the editor(s). MDPI and/or the editor(s) disclaim responsibility for any injury to people or property resulting from any ideas, methods, instructions or products referred to in the content.